

The Major Surface Carbohydrates of the *Echinococcus granulosus* Cyst: Mucin-Type O-Glycans Decorated by Novel Galactose-Based Structures[†]

Alvaro Díaz,^{*,‡} E. Carolina Fontana,[§] Adriane R. Todeschini,^{||} Silvia Soulé,[§] Humberto González,[§] Cecilia Casaravilla,[‡] Magdalena Portela,[⊥] Ronaldo Mohana-Borges,^{||} Lucia Mendonça-Previato,^{||} Jose O. Previato,^{||,‡} and Fernando Ferreira^{§,‡}

[‡]Cátedra de Inmunología, Departamento de Biociencias (Facultad de Química) e Instituto de Química Biológica (Facultad de Ciencias), Udelar, Montevideo, Uruguay, [§]Laboratorio de Carbohidratos y Glicoconjugados, Departamento de Química Orgánica, Facultad de Química/Facultad de Ciencias/Facultad de Medicina, Udelar, Montevideo, Uruguay, [⊥]Unidad de Proteómica y Bioquímica Analíticas, Instituto Pasteur y Facultad de Ciencias, Udelar, Montevideo, Uruguay, and ^{||}Instituto de Biofísica Carlos Chagas Filho, Universidade Federal do Rio de Janeiro, Cidade Universitária, 21949900, Rio de Janeiro, Brazil. [#]These authors contributed equally.

Received June 30, 2009; Revised Manuscript Received September 25, 2009

ABSTRACT: The cestodes constitute important but understudied human and veterinary parasites. Their surfaces are rich in carbohydrates, on which very little structural information is available. The tissue-dwelling larva (hydatid cyst) of the cestode *Echinococcus granulosus* is outwardly protected by a massive layer of carbohydrate-rich extracellular matrix, termed the laminated layer. The monosaccharide composition of this layer suggests that its major carbohydrate components are exclusively mucin-type O-glycans. We have purified these glycans after their release from the crude laminated layer and obtained by MS and NMR the complete structure of 10 of the most abundant components. The structures, between two and six residues in length, encompass a limited number of biosynthetic motifs. The mucin cores 1 and 2 are either nondecorated or elongated by a chain of Galpβ1–3 residues. This chain can be capped by a single Galpα1–4 residue, such capping becoming more dominant with increasing chain size. In addition, the core 2 N-acetylglucosamine residue is in cases substituted with the disaccharide Galpα1–4Galpβ1–4, giving rise to the blood P₁-antigen motif. Larger, also related, glycans exist, reaching at least 18 residues in size. The glycans described are related but larger than those previously described from an *Echinococcus multilocularis* mucin [Hulsmeier, A. J., et al. (2002) *J. Biol. Chem.* 277, 5742–5748]. Our results reveal that the *E. granulosus* cyst exposes to the host only a few different major carbohydrate motifs. These motifs are composed essentially of galactose units and include the elongation by (Galpβ1–3)_n and the capping by Galpα1–4, novel in animal mucin-type O-glycans.

The cestodes are obligate parasitic platyhelminths including medically and economically important genera such as *Echinococcus* and *Taenia* (family Taeniidae). Their study has lagged behind that of their sister parasitic platyhelminth taxon, the trematodes, which include the genus *Schistosoma*. Although transcriptomic and genomic data are now becoming available for some cestodes (www.sanger.ac.uk/cgi-bin/blast/submitblast/Echinococcus; LophDB in www.nematodes.org), glycomic data are very scarce (reviewed in ref 1). Carbohydrates are certainly central in the decoding of pathogens, including helminths, by the innate immune system. Usually for helminths, this decodification results in the instruction of adaptive responses that have a strong regulatory, noninflammatory, component (reviewed in ref 2). This is apparently the result of the evolutionary adaptation of these parasites to control the immune system. This adaptation reaches a high point in the taeniid cestodes, the larval stages of which can dwell in mammalian organ parenchymas for years without eliciting inflammation (reviewed in refs 3 and 4). Therefore, the surface carbohydrates of the larval taeniids are of

interest for understanding immune evasion by these parasites and also hold promise in the search for strategies to manipulate the immune system away from unwanted inflammatory responses (reviewed in ref 5).

Echinococcus granulosus, the causing agent of cystic hydatid disease, is a prime example of host inflammatory control. The larva or hydatid cyst, which can reach tens of centimeters in diameter in organ parenchymas of livestock and humans, usually thrives for years, surrounded by a noninfiltrated collagenous capsule, product of the resolution of the initial inflammation around the parasite (reviewed in refs 3 and 6). The hydatid cyst is a bladder-like, fluid-filled structure, bounded by the hydatid cyst wall. This wall comprises an inner, thin (10 μm) layer of parasite cells (germinal layer; GL)¹ and an outer, thick (up to a few millimeters), protective layer called the laminated layer (LL). The LL, laid out by the GL, is a specialized extracellular matrix present exclusively in the genus *Echinococcus*. It displays some variation in thickness and microscopic morphology among the different species (7), which include *Echinococcus multilocularis*, agent of the invasive alveolar hydatid disease (reviewed in refs 6 and 8). The major component of the LL in all *Echinococcus* species is an irregular meshwork of fibrils that is very rich in

[†]This work was supported by grants from the Universidad de la República (CSIC I + D no. 250/2002 and 404/2009) and from the Ministry of Education of Uruguay (PDT 54/078) and by an AMSUD-Pasteur travel grant to A.D.

^{*}To whom correspondence should be addressed. Tel/Fax: +59824874320. E-mail: adiaz@fq.edu.uy.

¹Abbreviations: GL, germinal layer; LL, laminated layer; PGC, porous graphitized carbon; CHCA, α-cyano-4-hydroxycinnamic acid.

carbohydrates (7, 9, 10). In addition, the *E. granulosus* LL contains abundant, nanometer-sized, deposits of a calcium salt of inositol hexakisphosphate (11–13).

The LL, in direct contact with the host, is widely thought to be the crucial element of the host–parasite interface in larval *Echinococcus* infections (8). Among several functions, the LL seems to contribute importantly to the induction of the noninflammatory response observed in *E. granulosus* infections in particular. This hypothesis is supported by the coincidence in time between the deployment of the LL by the establishing larva and inflammatory resolution and by the nonactivating properties of the LL when confronted in vitro with host complement or macrophages (3, 14–16).

In spite of its biological relevance, very little is known on the structure of the major, fibrillar component of the LL. However, when the available, fragmentary, information is put together, it suggests that these fibrils must be made up from mucins. Studies from the 1960s and 1970s showed that the *E. granulosus* LL contains galactose (Gal), *N*-acetylgalactosamine (GalNAc), and *N*-acetylglucosamine (GlcNAc), in decreasing order of abundance (17–20). The highly resistant LL dissolves when subjected to conditions of β -elimination (11, 17), a reaction typically undergone by O-linked glycans, and its hydrolysate contains a high level of threonine (18). Also, the transcriptome of the *E. granulosus* GL includes highly expressed, apparently tissue-specific sequences with characteristics of short apomucins, which bear C-terminal signals for addition of glycosylphosphatidylinositol anchors (Cecilia Fernández, personal communication; sequences EGC00317, EGC02904, EGC04254 in LophDB). In *E. multilocularis*, a mucin was purified from larval tissues by means of a monoclonal antibody (reactive with the LL), and its major O-glycans were characterized partially (21). In the present work, we elucidate in full the major glycans of the *E. granulosus* LL, starting from the crude structure. These are conventional core 1 and 2 O-glycans decorated with novel structures, based essentially only on galactose residues. They are related to the glycans partially elucidated for the *E. multilocularis* mucin, but they attain larger sizes.

EXPERIMENTAL PROCEDURES

Parasite Material. The starting material consisted of walls of *E. granulosus* hydatid cysts from natural infections in cattle. Cysts, usually from lung locations, were obtained from a plant in Uruguay dealing in offal products. Cyst walls were retrieved with the help of forceps after their collapse and detachment from the host organ that take place upon puncture of the normally turgent cysts and release of the hydatid cyst fluid. No attempt was made to separate the GL as this is not practical, and the contribution of the thin GL to the whole cyst wall material is quantitatively negligible. This material contains approximately 10% dry mass. The work in this paper was carried out on two batches of this starting material, each comprising a pool of several individual cysts; the two batches gave indistinguishable results.

Release of O-Glycans. Cyst walls (tens of grams wet mass) were extracted with 25 mM Tris-HCl, pH 7.5, containing 150 mM EDTA and 2 M NaCl (20 mL/g of wet mass). This treatment removes calcium inositol hexakisphosphate (13) and most of the adsorbed protein (22, 23). After a wash with water, cyst walls were subjected to reductive β -elimination by incubating for 5 days at 45 °C in 0.1 M NaOH and 0.3 M NaBH₄. This treatment caused the cyst walls to dissolve gradually, but a substantial insoluble residue remained. After centrifugation, the pellet was washed with 1 mL of water/g of wet mass, and the wash was pooled with the

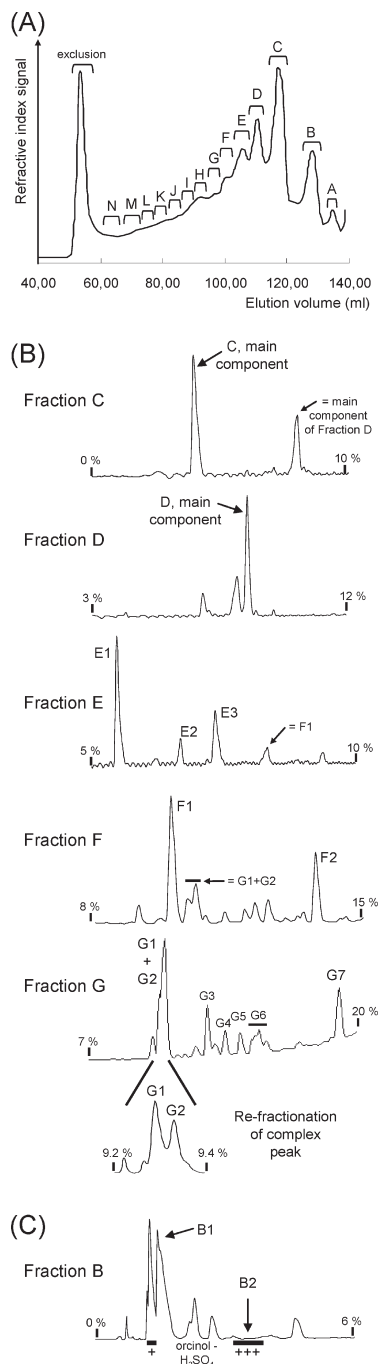


FIGURE 1: Purification summary. Oligosaccharide–alditols were fractionated by gel filtration on Bio-Gel P4 and then on the PGC column. Names for fractions and subfractions given are those used throughout the work. (A) Fractionation by gel filtration. (B) Subfractionation of five gel filtration fractions (containing conventional O-glycan-derived alditols) on the PGC column. Chromatographic profiles shown correspond to the absorption peak of the *N*-acetyl group (214 nm). In some cases, minor subfractions were judged to be identical to major ones from contiguous gel filtration fractions, as indicated. (C) Subfractionation on the PGC column of gel filtration fraction B, in which the main components lack the amide chromophore. The chromatogram corresponds to absorption at 205 nm (C–C double bond). Reactivity of eluted materials with orcinol–H₂SO₄ (general reaction for carbohydrates) was also tested, as indicated. In (B) and (C), indication of the percentual acetonitrile concentrations at which elution takes place has been given at the sides of each chromatogram.

supernatant. The resulting solution was neutralized with acetic acid and freeze-dried, and boric acid was removed by repeated

additions of methanol and evaporation to dryness. The residue was dissolved in water, passed through Dowex H⁺ resin (HCR-W2; Merck), and freeze-dried.

Purification of O-Glycans. Oligosaccharide–alditols were first purified on a Bio-Gel P4 (Bio-Rad) column (1.6 cm × 100 cm), eluted with 0.05 M acetic acid, using 10 mL/h flow rates and refractive index detection (Gilson 133). Between 100 and 200 mg of solid (of which 30–40% corresponded to oligosaccharide–alditols) was applied in each run. Gel filtration fractions, concentrated by freeze-drying, were then refractionated on a porous graphitized carbon (PGC) column (24) (Hypercarb, 7 μm, 4.6 mm bore × 20 cm; Thermo Fischer Scientific). Flow rates were 1 mL/min, and elution was carried out with linear water–acetonitrile gradients with the addition of 0.05% (v/v) trifluoroacetic acid; increasing acetonitrile concentrations were used for increasingly large products, as indicated beside each chromatogram in the Results section. UV detection at 214 nm was used except where specifically indicated. Up to 1.5 mg of carbohydrate was applied in each run, meaning that several runs were required for each gel filtration fraction. In some cases, poorly resolving peaks were refractionated in the same column.

Monosaccharide Analysis. This was carried out both by the alditol acetate method (25) (as described in detail in ref 11) and by the trimethylsilylated methyl glycoside method (26) (as described in detail in ref 27).

MALDI-TOF MS and MS-MS. Oligosaccharide–alditols were permethylated and processed for MALDI (28), but using α-cyano-4-hydroxycinnamic acid (CHCA) for the matrix instead of dihydroxybenzoic acid, as it yielded consistently better spectra (authors' unpublished observations). CHCA was dissolved at 10 mg/mL in 1 mM aqueous sodium acetate and mixed with equal volumes of the samples dissolved in methanol–water (1:1 v/v). One microliter volumes of the sample–matrix mixtures were spotted, air-dried, and recrystallized from 0.5 μL of ethanol–water (1:1 v/v). Spectra were obtained in the Applied Biosystems 4800 Analyzer MALDI-TOF-TOF at the Proteomics and Analytical Biochemistry Unit of the Institute Pasteur, Montevideo, Uruguay. Acquisition was in the positive reflector mode, in the *m/z* 400–4000 range. Spectra were externally calibrated using a mixture of peptide standards (4700 Cal Mix; Applied Biosystems). In some cases, internal calibration was performed, using the *m/z* value of a well-defined signal (permethylated oligosaccharide–alditol) common to several samples, and measured against the primary standard in a separate experiment carried out under the same conditions.

NMR. The smaller oligosaccharide–alditols (products from gel filtration fractions A–D) were analyzed on a Bruker AVANCE DPX 400 spectrometer (Facultad de Química, Udelar), equipped with a 5 mm QX probe and operating at ¹H and ¹³C frequencies of 400.13 and 100.61 MHz, respectively. All spectra were recorded in D₂O at 30 °C. ¹H and ¹³C chemical shifts were determined relative to the signals of TSP and acetone, respectively. The larger products (from gel filtration fractions E–G) were studied on a Bruker DMX 600 equipped with 5 mm triple resonance probe equipment at the Centro Nacional de Ressonância Magnética Nuclear, UFRJ, Brazil, and operating at ¹H and ¹³C frequencies of 600.22 and 150.93 MHz, respectively. All spectra were recorded in D₂O at 25 °C. ¹³C chemical shifts, determined from individual cross-peaks of the high-resolution 2D HSQC spectra, were calibrated using as internal standard the signal of the (*N*-acetamido)methyl group of the GalNAc-ol residue, taken to be invariable between the different products; this signal was in turn calibrated in one of the products against the

Table 1: MALDI-TOF Analysis of Permethylated Oligosaccharide–Alditols in Gel Filtration Fractions^a

fraction	measd mass	calcd mass	composition
B	493.24	493.26	HexHex-ol
C	534.26	534.29	HexHexNAc-ol
D	738.46	738.39	Hex ₂ HexNAc-ol
E	779.36	779.42	HexHexNAcHexNAc-ol
	942.44	942.49	Hex ₃ HexNAc-ol
F	983.46	983.52	Hex ₂ HexNAcHexNAc-ol
	1146.54	1146.59	Hex ₄ HexNAc-ol
G	1187.57	1187.61	Hex ₃ HexNAcHexNAc-ol
	1350.65	1350.69	Hex ₅ HexNAc-ol
H	1391.69	1391.71	Hex ₄ HexNAcHexNAc-ol
	1554.75	1554.79	Hex ₆ HexNAc-ol
I	1432.76	1432.74	Hex ₃ HexNAc ₂ HexNAc-ol
	1595.82	1595.81	Hex ₅ HexNAcHexNAc-ol
	1758.91	1758.89	Hex ₇ HexNAc-ol
	1963.02	1962.99	Hex ₈ HexNAc-ol
J	1636.82	1636.84	Hex ₄ HexNAc ₂ HexNAc-ol
	1799.90	1799.91	Hex ₆ HexNAcHexNAc-ol
K	1840.92	1840.94	Hex ₅ HexNAc ₂ HexNAc-ol
	2004.01	2004.01	Hex ₇ HexNAcHexNAc-ol
	2045.03	2045.04	Hex ₆ HexNAc ₂ HexNAc-ol
	2208.11	2208.11	Hex ₈ HexNAcHexNAc-ol
L	2249.12	2249.14	Hex ₇ HexNAc ₂ HexNAc-ol
	2412.19	2412.21	Hex ₉ HexNAcHexNAc-ol
	2453.22	2453.24	Hex ₈ HexNAc ₂ HexNAc-ol
M	2616.12	2616.31	Hex ₁₀ HexNAcHexNAc-ol
	2657.18	2657.34	Hex ₉ HexNAc ₂ HexNAc-ol
	2861.25	2861.44	Hex ₁₀ HexNAc ₂ HexNAc-ol
	3024.26	3024.51	Hex ₁₂ HexNAcHexNAc-ol
	3065.31	3065.54	Hex ₁₁ HexNAc ₂ HexNAc-ol
	3229.32	3228.61	Hex ₁₃ HexNAcHexNAc-ol
N	2902.14	2902.47	Hex ₉ HexNAc ₃ HexNAc-ol
	3106.29	3106.57	Hex ₁₀ HexNAc ₃ HexNAc-ol
	3310.41	3310.67	Hex ₁₁ HexNAc ₃ HexNAc-ol
	3473.45	3473.74	Hex ₁₃ HexNAc ₂ HexNAc-ol
	3514.48	3514.77	Hex ₁₂ HexNAc ₃ HexNAc-ol
	3555.51	3555.79	Hex ₁₁ HexNAc ₄ HexNAc-ol
	3718.48	3718.87	Hex ₁₃ HexNAc ₃ HexNAc-ol
	3759.67	3759.89	Hex ₁₂ HexNAc ₄ HexNAc-ol
	3963.65	3963.99	Hex ₁₃ HexNAc ₄ HexNAc-ol

^aThe fraction codes are as in Figure 1A. All masses correspond to monoisotopic values of Na⁺ adducts. Major signals, i.e., those showing at least 40% of the intensity of the single main signal in each fraction, are indicated in boldface. Signals that appear in more than one fraction are shown only for the fraction in which they have the highest relative abundance. Note that compositions of the type Hex_xHexNAc_yHexNAc-ol in cases may hide components of the type Hex_{x−1}HexNAc_{y+1}Hex-ol (see text and Supporting Information Table S1). Fraction A was not analyzed by MS, but it contains only galactitol by NMR (data not shown).

methyl carbon of acetone (30.89 ppm at 25 °C). ¹H NMR resonance assignments throughout the work were accomplished by standard two-dimensional experiments such as COSY, TOCSY, and/or NOESY. Gaussian resolution-enhancement window functions were employed to extract *J*-coupling data from broadened multiplets.

Methylation Analysis. This was carried out by permethylation, methanolysis, and acetylation, followed by GC-MS identification of the partially methylated acetylated methyl glycosides, as described previously (29).

RESULTS

The Laminated Layer Carbohydrates Are O-Glycans That Attain Large Sizes. The monosaccharide composition

Table 2: MALDI-TOF-TOF Analysis of Permethylylated Oligosaccharide—Alditols^a

fraction	measd mass	fragment ions	structure
B	493.2	259.1 (C ₁), 275.1 (Y ₁)	Hex-Hex-ol
C	534.3	259.2 (C ₁), 298.2 (Z ₁), 316.2 (Y ₁)	Hex-HexNAc-ol
D	738.5	259.1 (C ₁), 298.2 (Z ₁), 316.2 (Y ₁), 445.2 (B ₂), 463.2 (C ₂), 520.3 (Y ₂)	Hex-Hex-HexNAc-ol (identical to E2 by MS-MS)
E1	779.4	259.1 (C ₁), 282.1 (B _{1β}), 284.1 (Y _{1β} -Hex), 520.2 (Y _{1β}), 543.2 (Z _{1α}), 561.2 (Y _{1α})	Hex-(HexNAc)HexNAc-ol
E2	738.4	259.1 (C ₁), 298.2 (Z ₁), 316.2 (Y ₁), 445.2 (B ₂), 463.3 (C ₂), 520.3 (Y ₂)	Hex-Hex-HexNAc-ol (identical to D by MS-MS)
E3	942.5	259.1 (C ₁), 298.1 (Z ₁), 316.1 (Y ₁), 445.1 (B ₂), 463.2 (C ₂), 520.2 (Y ₂), 649.2 (B ₂), 667.3 (C ₃), 742.2 (Y ₃)	Hex-Hex-Hex-HexNAc-ol
F2	1146.6	259.1 (C ₁), 298.1 (Z ₁), 316.1 (Y ₁), 463.2 (C ₂), 520.2 (Y ₂), 649.2 (B ₃), 667.2 (C ₃), 724.2 (Y ₃), 853.2 (B ₄), 871.2 (C ₄), 928.3 (Y ₄)	Hex-Hex-Hex-Hex-HexNAc-ol
G1	1187.6	259.2 (C _{1α} /C _{1β}), 284.1 (Y _{1α} -Hex), 463.2 (C _{2α}), 520.2 (Y _{1α}), 529.2 (Y _{2α} -Hex), 690.2 (B _{3α}), 733.3 (Y _{3α} -Hex), 765.3 (Y _{2α}), 951.3 (Z _{1β}), 969.3 (Y _{3α})	Hex-(Hex-Hex-HexNAc)HexNAc-ol
G2	1187.6	259.1 (C _{1α}), 282.1 (B _{1β}), 284.1 (Y _{1β} -Hex ₃), 463.2 (C _{2α}), 520.2 (Y _{1α} from G1), 543.2 (Z _{1α}), 561.2 (Y _{1α} from G1), 690.2 (B _{3α} from G1), 765.3 (Y _{2α}), 912.3 (Z _{1β}), 928.3 (Y _{1β}), 951.3 (Z _{1β} from G1), 969.3 (Y _{3α})	Hex-Hex-Hex-(HexNAc)HexNAc-ol (+contamination with product G1)

^aThe codes correspond to gel filtration fractions (B, C, D) or PGC subfractions (all the rest) shown in Figure 1. Note that the MS-MS data for products F1, G3, and G7 are presented in graphic form in Figure 2. All masses correspond to monoisotopic values of Na⁺ adducts. Masses listed are experimental ones, and they correspond to the expected masses to within 0.1 Da for pseudomolecular ions and to within 0.3 Da for fragments. Fragment ions listed correspond to the signals of higher relative intensity and/or particular diagnostic value. Names of fragments follow the nomenclature of Domon and Costello (48), with the alditol residue having been assigned the subscript 1. Structures listed correspond to deductions based on MS data only. Note that the favored generation of B-type ions by cleavage at position 1 of HexNAc residues and of Z-type ions by cleavage at position 3 (determined on the basis of data in Tables 3 and 4) of HexNAc-ol residues both involve the loss of a water molecule. B-type ions also arise from cleavage at position 1 of hexose residues, though more weakly. Also note that the loss of substituents linked through the anomeric carbon of HexNAc or linked to C-2 of HexNAc or HexNAc-ol also gives rise to internal fragmentations, indicated as “Y_{1β}-Hex”, etc.

of the crude cyst wall (depleted of inositol hexakisphosphate) was found, both by the alditol acetate and by the trimethylsilylated methyl glycoside methods, to be only Gal, GalNAc, and GlcNAc in decreasing order of abundance (not shown), confirming the previous reports (17–20). This composition and, in particular, the absence of detectable mannose indicate that the bulk of the LL carbohydrates consists of O-linked glycans, rather than N-linked glycans. In addition, as the parasite cells must contain N-linked glycoproteins, this monosaccharide composition also confirms that the thin GL contributes a negligible amount of material to the crude cyst wall. By the alditol acetate analysis with the use of a rhamnose internal standard, the three major monosaccharides were estimated to account for 33% of the cyst wall dry mass (Gal, 19%; GalNAc, 11%; GlcNAc, 3%; approximate molar ratio 7:3:1). Approximately 35% of the cyst wall dry mass corresponds to calcium inositol hexakisphosphate (12); apomucins, nonmucin proteins including adsorbed, non-LL-intrinsic proteins, salts, and possibly lipids must make up the remainder of the dry mass.

The *E. granulosus* LL cannot be solubilized without rather drastic treatments. A combination of disulfide reduction and sonication affords almost complete solubilization, but the resulting material consists of very high molecular mass aggregates and is not amenable to conventional purification procedures (C. Casaravilla and A. Diaz, unpublished results). We therefore chose to release, purify, and elucidate the O-glycans starting with the crude, insoluble cyst wall, a strategy allowing unbiased assessment of the major carbohydrate components of the LL. Thus whole cyst walls were washed so as to eliminate inositol hexakisphosphate and (most) adsorbed protein and then subjected to prolonged reductive β-elimination. The desalted supernatant was separated by gel filtration on Bio-Gel P4 column, giving a complex profile of oligosaccharide—alditols (Figure 1A). The yield of released O-glycans (fractions B–N, Figure 1A) was approximately 18% of the initial cyst wall dry mass, as determined by weighing the purified fractions. It must be stressed that, even after the 5 days employed, the β-elimination reaction was not complete. In addition to material in the column void volume (3.4% of initial dry mass), a substantial insoluble residue remained at the end of the alkaline treatment. Although this residue could be dissolved in water (as opposed to the reaction medium containing NaBH₄ and NaOH), it eluted in the Bio-Gel P4 void volume, even when chromatographed in the presence of 4 M urea. When subjected to a second round of reductive β-elimination, a much smaller residue was left, and the supernatant showed upon gel filtration a profile of oligosaccharide—alditols that was very similar to the initial one.

The gel filtration fractions were subjected to permethylation and MALDI-TOF MS analysis (Table 1). The results were compatible with the presence of O-glycans with the overall composition suggested by the monosaccharide analysis of the crude cyst wall. Oligosaccharide—alditols made up from up to 18 residues (including the alditol residue) were unequivocally detected. The O-linked oligosaccharide—alditols contained between 0 and 4 HexNAc residues (excluding the reduced end HexNAc-ol), the number of HexNAc residues generally increasing with glycan size. Fraction A was found by NMR (not shown) to consist of galactitol, while fraction B appeared to contain glycan(s) lacking the expected HexNAc-ol, as confirmed by further data presented below.

The Two Major Glycans in the Laminated Layer Are Truncated Core 1 and Core 1 Elongated by Galactose

Table 3: Linkage Analysis of Selected Purified Products

fraction	result of linkage analysis
C	terminal Galp, 3-subst GalNAc-ol
D	terminal Galp, 3-subst Galp, 3-subst GalNAc-ol (+terminal GlcNAcp)
E1	terminal Galp, terminal GlcNAcp, 3,6-disubst GalNAc-ol
E3	terminal Galp, 4-subst Galp, 3-subst Galp, 3-subst GalNAc-ol
F1	terminal Galp, 3-subst Galp, terminal GlcNAcp, 3,6-disubst GalNAc-ol
F2	terminal Galp, 3-subst Galp, 4-subst Galp, 3-subst GalNAc-ol
G1	terminal Galp, 4-subst Galp, 4-subst GlcNAcp, 3,6-disubst GalNAc-ol
G7	terminal Galp, 3-subst Galp, 4-subst Galp, 3-subst GalNAc-ol

^aThe 3,6-disubstituted GalNAc-ol residues were evidenced by the appearance of 1,4,5-trimethyl-, *N*-methyl-, and 3,6-anhydro-*N*-acetylgalactosaminitol, identifiable by its MS fragmentation pattern (49). No attempt was made to determine molar ratios between the different partially methylated acetylated methyl glycosides obtained as significant components. A significant amount of terminal GlcNAc in fraction D probably arises from a contaminating product, as this material was not purified on the PGC column before analysis.

β 1–3. The gel filtration profile displayed two major oligosaccharide–alditol peaks (peaks C and D in Figure 1A), each of which in turn displayed a single dominant peak on analytical runs on the PGC column (Figure 1B). These two major components were elucidated by NMR, MS-MS, and methylation analysis as Galp β 1–3GalNAc-ol and Galp β 1–3Galp β 1–3GalNAc-ol, respectively (Tables 2, 3, and 4). Hence the two major glycans in the LL are the nondecorated conventional core 1 of animal mucins (Galp β 1–3GalNAcp α -Ser/Thr) and core 1 decorated with a single Galp β 1–3 residue.

Additional O-Glycans Are Formed by the Elongation and Capping of Cores 1 and 2 with Galactose Units. Gel filtration fractions eluting before peak D gave complex profiles upon PGC HPLC (Figure 1B). Nine oligosaccharide–alditols, corresponding to the major HPLC peaks obtained upon subfractionation of gel filtration fractions E, F, and G, were elucidated as above (Tables 2, 3, and 4 and Figure 2). Four of these corresponded to linear O-glycans: Galp β 1–3Galp β 1–3GalNAc-ol (fraction E2, identical to the major component in fraction D, above), Galp α 1–4Galp β 1–3Galp β 1–3GalNAc-ol (fraction E3), Galp α 1–4Galp β 1–3Galp β 1–3Galp β 1–3GalNAc-ol (fraction F2), and Galp α 1–4Galp β 1–3Galp β 1–3Galp β 1–3Galp β 1–3GalNAc-ol (fraction G7). Therefore, this linear series can be rationalized as the result of the elongation of core 1 with one to three Galp β 1–3 residues and the addition, after the first such elongation step, of a Galp α 1–4 “cap”. The simplest branched structure (E1) was Galp β 1–3(GlcNAcp β 1–6)GalNAc-ol, i.e., the derivative of O-glycan core 2. Another branched component corresponded to the product of decoration of the Gal residue of this core with a Galp β 1–3 residue: Galp β 1–3Galp β 1–3(GlcNAcp β 1–6)GalNAc-ol (F1). A further structure corresponded to the addition of a Galp α 1–4 cap onto the previous one: Galp α 1–4Galp β 1–3Galp β 1–3(GlcNAcp β 1–6)GalNAc-ol (G2). Finally, two other structures were related to E3 and F1 by the addition of a Galp α 1–4Galp β 1–4 motif on the core 2 GlcNAc unit: Galp β 1–3(Galp α 1–4Galp β 1–4GlcNAcp β 1–6)GalNAc-ol (G1) and Galp β 1–3Galp β 1–3(Galp α 1–4Galp β 1–4GlcNAcp β 1–6)GalNAc-ol (G3).

Minor oligosaccharide–alditols, either from less conspicuous chromatographic peaks (Figure 1) or appearing as contaminants of the major structures described above, were analyzed by MS-MS (Supporting Information Table S1). Whenever it was possible to interpret their fragmentation spectra, these products appeared to comprise the same structural motifs present in the fully elucidated oligosaccharide–alditols, i.e., the elongation of cores 1 and 2 with a variable number of Hex (Gal) residues added

onto either core’s Gal residue, and the possibility of decoration of the HexNAc (GlcNAc) unit of core 2 with two Hex (Gal) residues. The component with $M_r = 1187.6$ in fraction G6, deduced to be Hex-Hex-Hex-(HexNAc)HexNAc-ol, must be, by virtue of its chromatographic retention time (Figure 1), a linkage isomer of G2; the most parsimonious possibility is that the component in G6 is the cap-less isomer, Galp β 1–3Galp β 1–3Galp β 1–3(GlcNAcp β 1–6)GalNAc-ol. In addition, a contaminant in fraction G2 ($M_r = 1228.6$) contributed initial evidence of a motif not gleaned from the other data, namely, the ramification of the Hex (Gal) residue of core 2 with a HexNAc residue. Also of note, two minor components (fraction G4; $M_r = 1350.7$ and 1554.8) had Hex-ol reducing ends. These probably arise from the loss of the reducing terminal GalNAc in peeling reactions during the prolonged β -elimination, followed by the reduction of the newly formed reducing end. This assumption made, these two products hint that different residues along the linear Hex (Gal) chain starting at the core can be ramified with HexNAc residues, which may turn be decorated with two Hex (presumably Gal) residues, in apparent similarity to the core 2 GlcNAc residue. Taken together, the structural data (either complete or partial) for the components present in the PGC subfractions of gel filtration fractions E, F, and G (Tables 2, 3, and 4 and Supporting Information Table S1; Figure 2) are fully consistent with the MS data obtained for the same gel filtration fractions without further purification (Table 1).

The late-eluting gel filtration fraction B, which by MS appeared to contain a product with the composition Hex-Hex-ol (Table 1), yielded only galactitol acetate as conventional product after monosaccharide analysis by the alditol acetate method. By NMR, it appeared to consist of an approximately equimolar mixture of a product with the general composition Gal-Gal-ol and a smaller product containing a C–C double bond. The fraction was thus subfractionated on the PGC column using UV detection at 205 nm and general carbohydrate detection by the orcinol–sulfuric acid reaction on aliquots of the eluted fractions (Figure 1C). One of its major components (B2), giving a positive orcinol–sulfuric acid reaction and not absorbing at 205 nm, was identified by NMR as Galp β 1–3/ β 1–4Gal-ol (diastereomeric pair not discriminated by NMR; Supporting Information Table S2) and likely arises from peeling reactions. The other major component of fraction B (peak B1 in Figure 1), not giving carbohydrate reactivity and absorbing strongly at 205 nm (but not at 214 nm, not shown), was found to be a double bond-containing derivative of a hexitol (Supporting Information Table S2). This product may result from the base-catalyzed

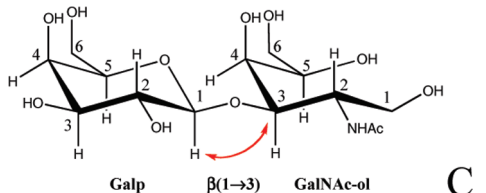
dehydration of galactose (through a 3-deoxygalactosone intermediate (30)), followed by borohydride-mediated reduction. The free galactose is probably the product of peeling reactions and also generates the galactitol found in fraction A.

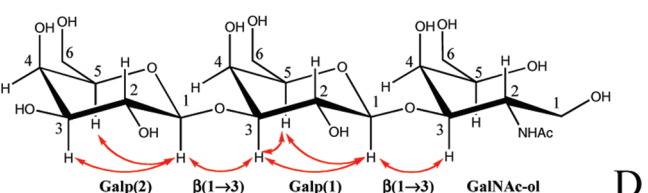
DISCUSSION

We have tackled the carbohydrate components of the *E. granulosus* LL, obtaining data that are fully consistent with the notion that the fibrillar meshwork of this extracellular matrix is made up from mucins. We thus have determined that the major LL carbohydrates are *O*-glycans based on conventional

mucin-type cores 1 and 2 and have described in full their most abundant members, which have between two and six residues in length. Further, we have determined the existence in the LL of additional *O*-glycans up to 18 residues in length. It must be noted that cattle, a practical source of *E. granulosus* material in Uruguay, is not an appropriate host for the most prevalent (sheep) strain of the parasite. Therefore, cattle cysts most often display decreased vitality, associated with a nonresolving host granulomatous reaction (23). It is thus important to determine if the preponderance of small LL glycans observed in this work (Figure 1A) is fully representative of the hydatid cyst in appropriate hosts.

Table 4: NMR Assignments of Oligosaccharide–Alditols^a

<div><div>Galp β(1→3) GalNAc-ol C</div></div>															
chemical shift (ppm)															
residues	H-1	H-2	H-3	H-4	H-5	H-6	H-6'	NAc	C-1	C-2	C-3	C-4	C-5	C-6	NAc
GalNAc-ol	3.73, 3.78	4.40	4.07	3.52	4.20	3.64	3.69	2.06	61.0	51.9	76.8	69.5	69.8	63.3	22.3, 175.1
Galp	4.45 (7.8)	3.57	3.68	3.91	3.74	3.79	3.79		104.4	71.5	72.9	69.0	75.5	61.5	

<div><div>Galp(2) β(1→3) Galp(1) β(1→3) GalNAc-ol D</div></div>															
chemical shift (ppm)															
residues	H-1	H-2	H-3	H-4	H-5	H-6	H-6'	NAc	C-1	C-2	C-3	C-4	C-5	C-6	NAc
GalNAc-ol	3.75, 3.80	4.40	4.09	3.53	4.19	3.65	3.68	2.06	61.0	51.9	76.8	69.5	69.8	63.3	22.3, 175.1
Galp(1)	4.55 (7.8)	3.73	3.84	4.18	3.69	3.76	3.76		104.0	70.7	82.4	68.8	75.1	61.4	
Galp(2)	4.62 (7.4)	3.61	3.65	3.94	3.68	3.76	3.76		104.8	71.5	73.0	69.0	75.5	61.4	

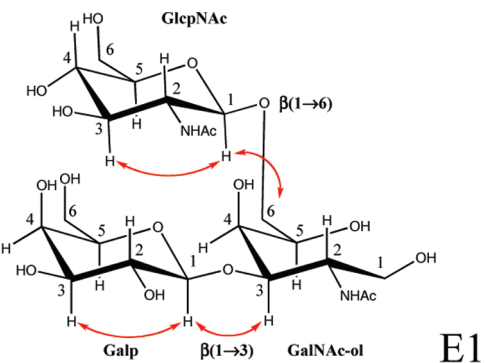
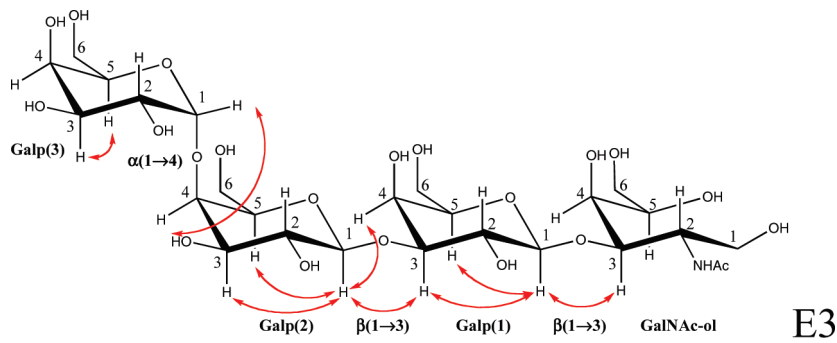
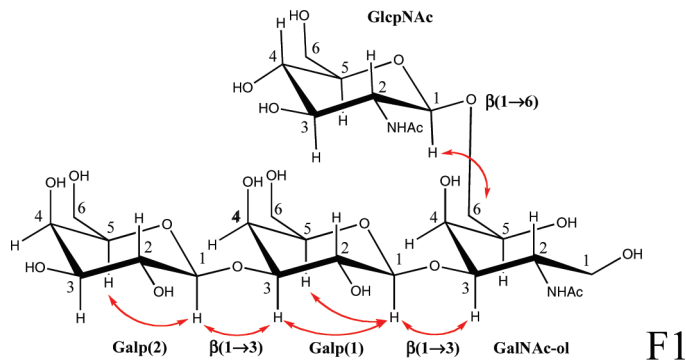
<div><div>GlcNAc β(1→6) Galp β(1→3) GalNAc-ol E1</div></div>															
chemical shift (ppm)															
residues	H-1	H-2	H-3	H-4	H-5	H-6	H-6'	NAc	C-1	C-2	C-3	C-4	C-5	C-6	NAc
GalNAc-ol	3.74, 3.80	4.42	4.08	3.45	4.31	3.67	3.94	2.08	61.2	51.9	76.3	69.1	67.8	71.2	22.7
GlcNAc	4.54 (8.4)	3.72	3.52	3.45	3.46	3.76	3.94	2.08	102.3	56.0	74.4	70.3	76.4	61.2	22.7
Galp	4.47 (7.9)	3.57	3.67	3.89	3.73	3.78	— ^b		104.4	71.6	73.0	68.9	75.4	61.5	

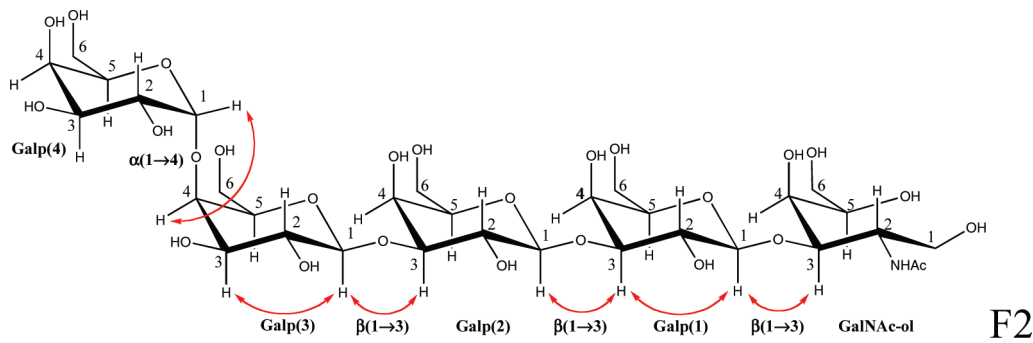
Table 4. Continued



residues	chemical shift (ppm)														
	H-1	H-2	H-3	H-4	H-5	H-6	H-6'	NAc	C-1	C-2	C-3	C-4	C-5	C-6	NAc
GalNAc-ol	3.76, 3.80	4.42	4.10	3.51	4.22	3.64	3.68	2.06	61.7	52.2	76.9	69.5	70.0	63.7	22.7
Galp(1)	4.55 (7.9)	3.75	3.89	4.17	3.77	3.78	— ^b		102.3	56.0	74.4	70.3	76.4	61.2	
Galp(2)	4.71 (7.7)	3.66	3.76	4.05	3.77	3.85	3.89		105.4	71.6	72.8	78.0	75.7	60.9	
Galp(3)	4.96 (3.7)	3.84	3.93	4.03	4.41	3.71	— ^b		100.9	69.4	69.9	69.7	71.5	61.	

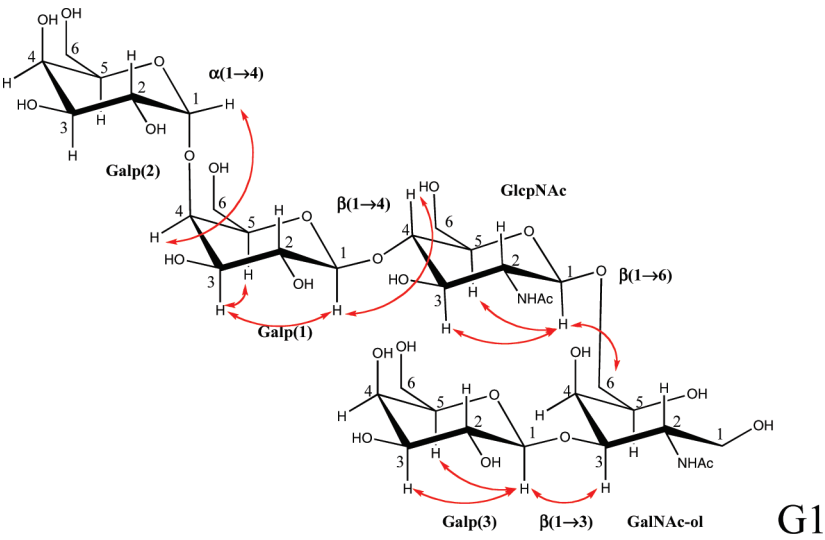


residues	chemical shift (ppm)														
	H-1	H-2	H-3	H-4	H-5	H-6	H-6'	NAc	C-1	C-2	C-3	C-4	C-5	C-6	NAc
GalNAc-ol	3.75, 3.79	4.41	4.09	3.47	4.29	3.69	3.94	2.07	61.2	52.0	76.5	69.1	67.8	71.1	22.7
GlcNAc _p	4.55 (8.4)	3.72	3.53	3.45	3.46	3.75	3.94	2.07	103.0	56.7	75.1	71.0	77.1	61.9	22.7
Galp(1)	4.54 (7.8)	3.73	3.85	4.20	3.76	3.79	— ^b		104.1	70.8	82.6	68.9	75.1	61.2	
Galp(2)	4.62 (7.7)	3.63	3.67	3.93	3.70	3.75	— ^b		104.9	71.6	73.0	69.1	75.6	61.2	

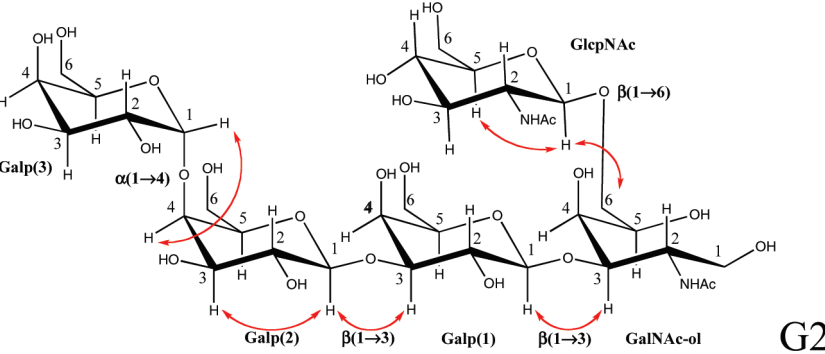


residues	chemical shift (ppm)														
	H-1	H-2	H-3	H-4	H-5	H-6	H-6'	NAc	C-1	C-2	C-3	C-4	C-5	C-6	NAc
GalNAc-ol	3.74, 3.81	4.41	4.09	3.52	4.21	3.64	3.68	2.05	61.3	52.0	76.6	69.4	69.7	63.4	22.7
Galp(1)	4.55 (7.9)	3.74	3.89	4.20	3.77	3.78	— ^b		103.9	70.8	82.3	69.1	75.5	61.3	
Galp(2)	4.68 (7.7)	3.80	3.89	4.17	3.72	3.78	— ^b		104.5	70.8	82.3	69.1	75.2	61.3	
Galp(3)	4.71 (7.8)	3.65	3.74	4.05	3.77	3.85	3.90		105.0	71.5	72.8	77.8	75.5	60.6	
Galp(4)	4.97 (3.8)	3.84	3.93	4.04	4.39	3.72	— ^b		100.8	69.2	69.7	69.5	71.4	61.3	

Table 4. Continued

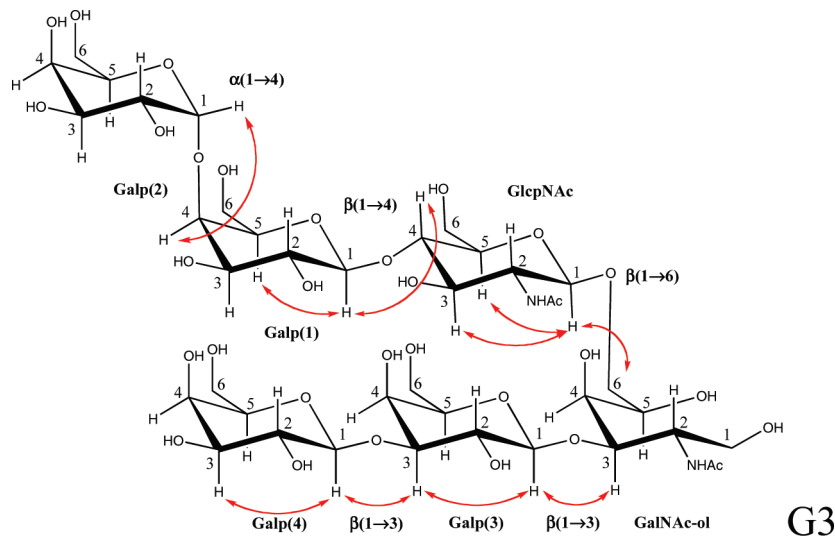


residues	chemical shift (ppm)														
	H-1	H-2	H-3	H-4	H-5	H-6	H-6'	NAc	C-1	C-2	C-3	C-4	C-5	C-6	NAc
GalNAc-ol	3.76, 3.79	4.41	4.07	3.47	4.29	3.69	3.94	2.08	61.1	52.1	76.6	69.3	67.9	71.3	22.7
GlcNAc _p	4.57 (8.4)	3.76	3.68	3.72	3.60	3.85	4.02	2.08	102.2	55.8	73.1	79.4	75.4	60.7	22.7
Galp(1)	4.54 (7.8)	3.59	3.75	4.05	3.79	3.76	3.92		103.9	71.6	72.8	77.9	76.0		
Galp(2)	4.95 (3.9)	3.84	3.90	4.04	4.37	3.72	— ^b		100.9	69.2	69.3	69.5	71.4	61.1	
Galp(3)	4.48 (7.8)	3.57	3.68	3.90	3.72	3.80	— ^b		104.6	71.6	73.1	69.3	75.6	61.1	

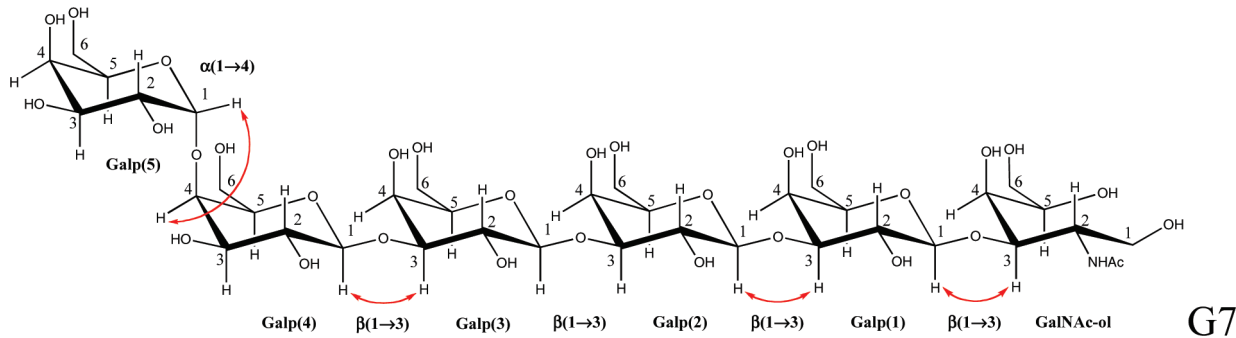


residues	chemical shift (ppm)														
	H-1	H-2	H-3	H-4	H-5	H-6	H-6'	NAc	C-1	C-2	C-3	C-4	C-5	C-6	NAc
GalNAc-ol	3.75, 3.80	4.41	4.09	3.47	4.29	3.68	3.94	2.08	61.2	52.0	76.6	69.4	68.0	71.2	22.7
GlcNAc _p	4.55 (8.4)	3.72	3.53	3.45	3.46	3.75	3.95	2.08	102.4	56.0	74.5	70.4	76.4	61.3	22.7
Galp(1)	4.54 (7.7)	3.75	3.87	4.16	3.78	3.78	— ^b		104.1	71.1	82.5	68.9	75.8	61.3	
Galp(2)	4.70 (7.7)	3.66	3.75	4.05	3.74	3.85	3.89		105.1	71.6	72.8	77.9	75.3	60.8	
Galp(3)	4.98 (3.9)	3.85	3.92	4.05	4.39	3.72			100.9	69.2	69.6	69.6	71.5	61.2	

Table 4. Continued



residues	chemical shift (ppm)														
	H-1	H-2	H-3	H-4	H-5	H-6	H-6'	NAc	C-1	C-2	C-3	C-4	C-5	C-6	NAc
GalNAc-ol	3.76, 3.81	4.41	4.09	3.48	4.29	3.70	3.94	2.08	61.5	52.0	76.5	69.2	67.9	71.1	22.7
GlcNAc	4.57 (8.5)	3.76	3.71	3.72	3.61	3.87	4.03	2.08	102.2	55.6	73.1	79.3	75.3	60.7	22.7
Galp(1)	4.54 (7.8)	3.58	3.76	4.06	3.80	3.80	3.92		104.0	71.5	72.8	77.9	76.0	60.9	
Galp(2)	4.96 (3.9)	3.85	3.91	4.04	4.37	3.72	— ^b		100.9	69.1	69.6	69.5	71.3	61.1	
Galp(3)	4.54 (7.8)	3.74	3.85	4.20	3.76	3.76	— ^b		104.0	70.8	82.6	68.8	75.2	61.1	
Galp(4)	4.62 (7.6)	3.63	3.69	3.94	3.71	3.80	— ^b		104.9	71.6	73.1	69.2	75.6	61.1	



residues	chemical shift (ppm)														
	H-1	H-2	H-3	H-4	H-5	H-6	H-6'	NAc	C-1	C-2	C-3	C-4	C-5	C-6	NAc
GalNAc-ol	3.75, 3.80	4.40	4.09	3.51	4.20	3.64	3.68	2.05	61.2	52.1	77.0	69.7	69.9	63.6	22.7
Galp(1)	4.54 (7.9)	3.75	3.87	4.19	3.77	3.76	— ^b		104.2	71.0	82.6	69.1	75.5	61.6	
Galp(2)	4.69 (7.8)	3.80	3.87	4.21	3.72	3.76	— ^b		104.6	71.0	82.6	69.1	75.4	61.6	
Galp(3)	4.69 (7.8)	3.80	3.87	4.17	3.72	3.76	— ^b		104.6	71.0	82.6	69.1	75.4	61.6	
Galp(4)	4.71 (7.7)	3.65	3.75	4.04	3.77	3.85	3.90		105.0	71.7	72.9	78.0	75.6	61.0	
Galp(5)	4.97 (3.2)	3.85	3.91	4.04	4.38	3.71	— ^b		101.0	69.3	69.8	69.7	71.4	61.4	

^aExcept for structures C and D, ¹³C shifts were obtained from HSQC spectra, and hence the shifts of the carbonyl carbons could not be obtained. Coupling constants are given in parentheses for H-1 atoms of monosaccharide residues only. Correlations are indicated with arrows on the structures; these were derived from NOE spectra (NOESY, ROESY, or TROESY), except for product C (from HMBC). Spectral data for products E2 and D were indistinguishable (same compound). ^bChemical shift values could not be obtained due to signal superimposition.

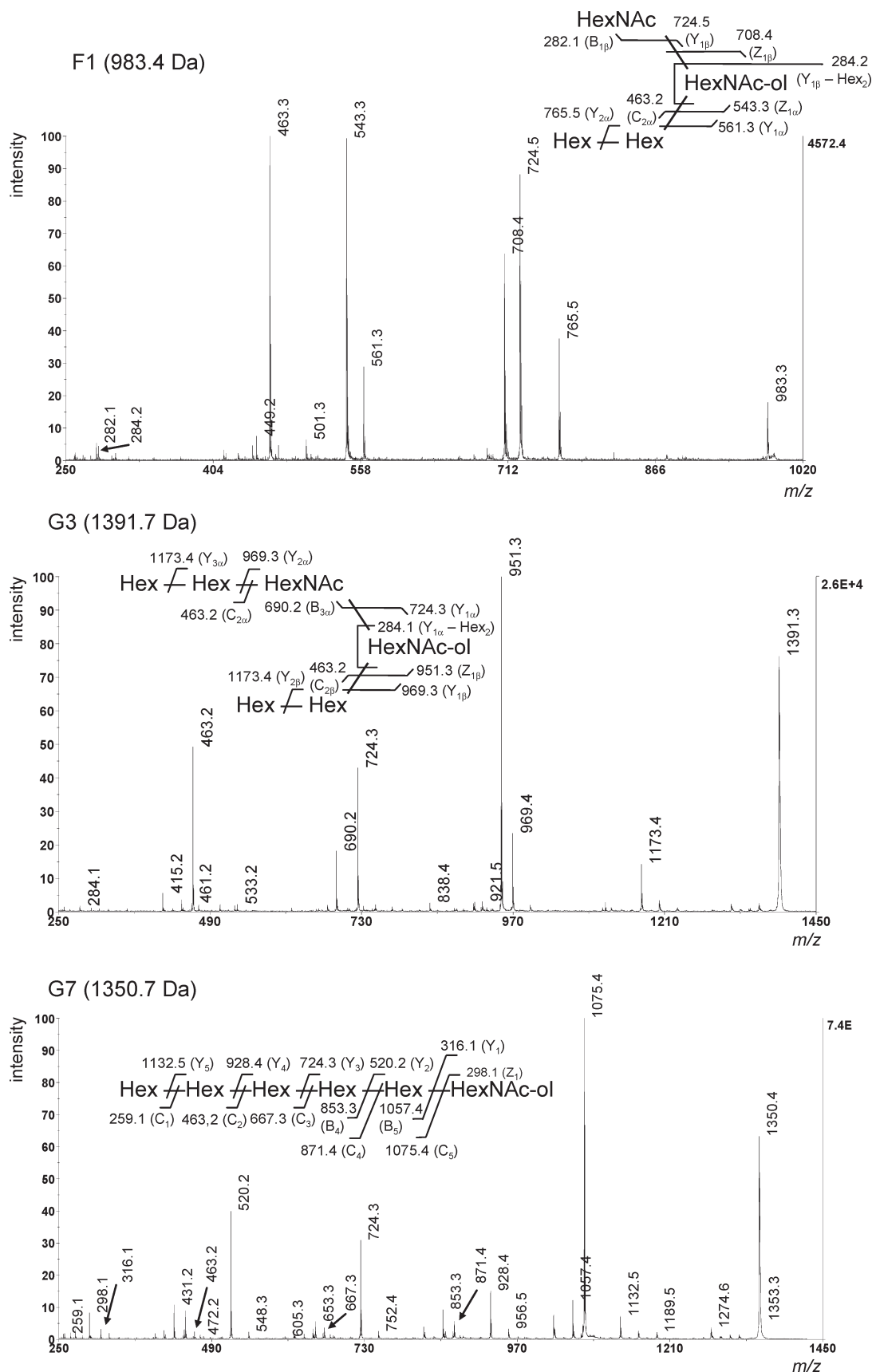


FIGURE 2: Assignments by MALDI-TOF-TOF MS-MS of representative permethylated oligosaccharide—alditols. All specifications given in the legend to Table 2 apply.

The ten structures of complete *O*-glycans elucidated in this work are summarized in Figure 3 and can be rationalized on the basis of a few simple motifs. The conventional cores 1 and 2 can

be nondecorated (structures C and E1). Alternatively, they can be elongated with one to three Galp β 1–3 units added onto the core Galp β 1–3 residue. The resulting Galp β 1–3 chain can be

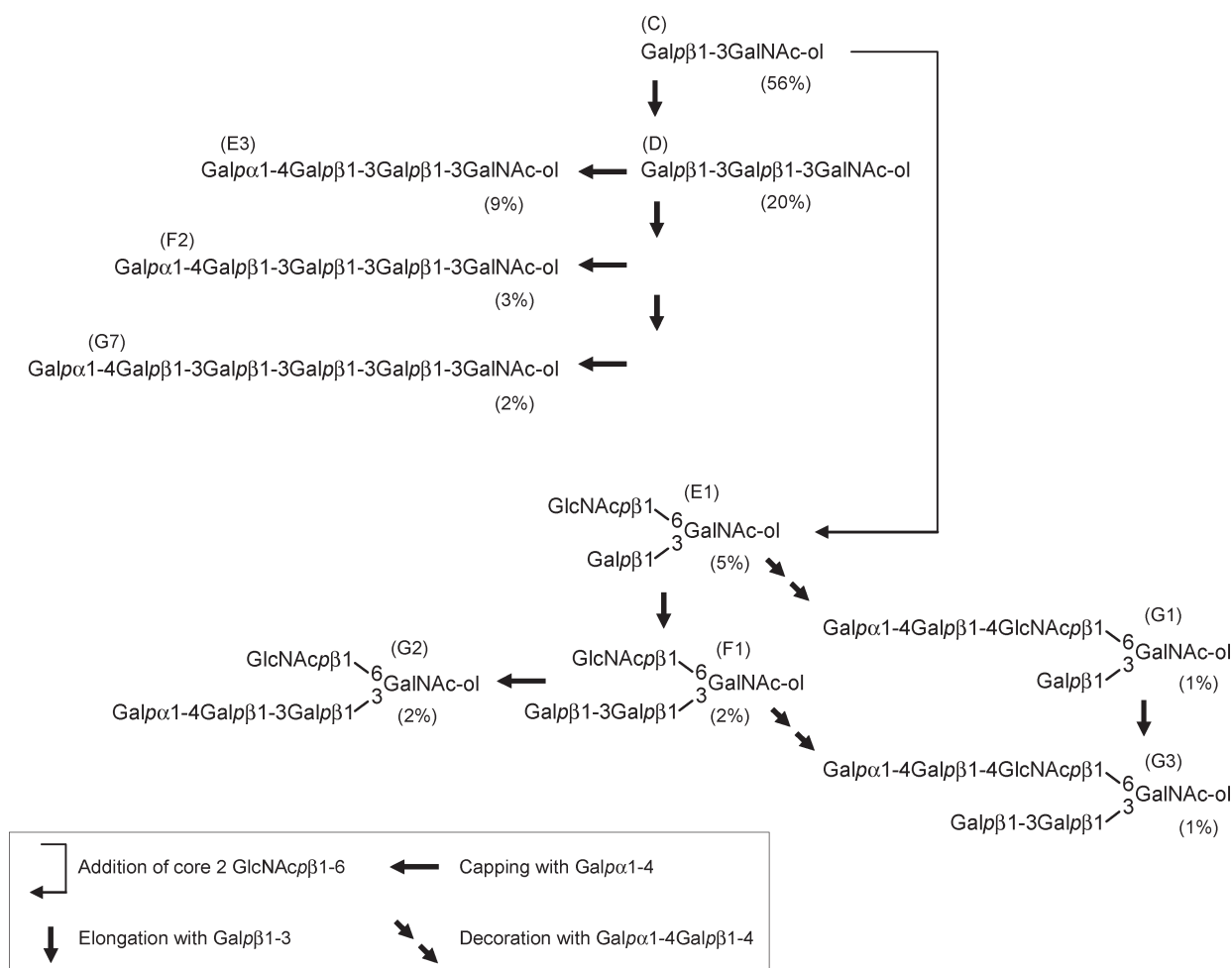


FIGURE 3: Summary of fully elucidated oligosaccharide-alditol structures. Codes are as in Figure 1. Possible biosynthetic relationships between the respective parent *O*-glycans (which may be assumed to be attached to apomucin backbones by GalNAcα1-Ser/Thr linkages) are indicated. Estimated abundances are given in parentheses (mol % with respect to the total abundance of the fully elucidated glycans). Abundances were estimated by pooling gel filtration fractions B–N (Figure 1), running the mixture on the PGC column using a linear 5–20% acetonitrile gradient and detection at 206 nm (other conditions as in Experimental Procedures), identifying the components by use of the pure products as standards, integrating peak areas, and normalizing these by the number of *N*-acetyl groups known to be present in each product.

terminated as such (structures D, F1, and G3) or with the addition of a single Galpα1-4 acting as a cap (structures E3, F2, G2, and G7). Elongation by Galpβ1-3 chains and capping by Galpα1-4 are to our knowledge novel on *O*-glycans. Neither structural feature is known in *Echinococcus* glycolipids (31), although Galpα1-4Gal termini are known in glycosphingolipids from certain other cestodes (reviewed in ref 1). *Echinococcus* *N*-glycans (32) do not seem to feature the Galpβ1-3 elongation, while Galpα1-4Gal termini are likely present, but in the context of the P₁-antigen, discussed next. The other major motif found in the LL carbohydrates is the decoration of some core 2-based *O*-glycans with Galpα1-4Galpβ1-4 on the core GlcNAc residue (structures G1 and G3; Figure 3). The resulting Galα1-4Galβ1-4GlcNAcβ structure corresponds to the P₁ blood group motif, explaining the long-known P₁ reactivity present in the LL (20, 33, 34). The P₁ motif is very likely carried also on *E. granulosus* *N*-glycans (from partial structural data (32)), as well as on glycosphingolipids (from immunoreactivity (35)); in contrast, in mammals it is found in glycolipids only (reviewed in ref 36). Overall, Galpβ1-3 elongation may well be specific of the *O*-glycans of the *Echinococcus* LL, while in contrast capping with Galpα1-4 (which includes, but is not limited to, the context giving rise to the P₁ motif) may be a widespread

feature of cestode *O*- and *N*-glycans and glycolipids, as previously suggested (1).

The structural motifs discussed above might be sufficient to explain all those glycan compositions detected in the LL by MS (Table 1), except for those that include two, three, or four HexNAc residues outside the reducing end. These latter may be explained by the additional HexNAc-containing ramifications gleaned from some of the partially elucidated structures (Supporting Information Table S1); examples of such glycans are being presently elucidated. In addition, the evidence from MS of compositions Hex_{6–8}HexNAc-ol (Table 1) suggests that the Galpβ1-3 elongation can proceed through at least six residues (assuming one Gal residue in the core and another in the cap). Globally, the picture arising from our study is one of striking structural simplicity. In addition, it is sharply different from the picture from the only glycobiologically well-studied platyhelminth, *Schistosoma mansoni*. Indeed, in contrast to *S. mansoni* carbohydrates and *O*-glycans in particular (reviewed in ref 37), the LL glycans lack lactosamine or LacDiNAc termini and, crucially, lack fucosylation.

The enzyme presumably responsible for the first step of the synthesis of the *O*-glycans described in this work, an UDP-GalNAc:polypeptide GalNAc transferase expressed in the *E. granulosus* GL, has been characterized (38); a second sequence

with similarity to the same class of enzymes is also present in the GL transcriptome (EGC04989). This transcriptome (C. Fernández, personal communication) also contains two sequences with similarities to core 1 β 1–3 galactosyltransferases (EGC01546, EGC04121), and a sequence similar to β 1–4 galactosyltransferases (EGC00364). Also, probably reflecting the central importance of Gal in the biosynthesis of the LL, several hits in ca. 1500 total clusters correspond to sequences of proteins probably involved in the synthesis of UDP-Gal and its translocation across Golgi membranes (EGC01356, EGC00902, EGC00933).

The structures reported in this work should be compared with those reported by Hulsmeier et al. for the purified *E. multilocularis* mucin (21). Although anomeric configurations were not determined in that work, the data are clearly consistent with structures based on cores 1 and 2, with the nondecorated cores constituting the two most abundant glycans. Nondecorated core 1 is probably expressed strongly in the LL across the genus *Echinococcus*, as peanut agglutinin and jacalin bind readily to the entire LLs of *E. multilocularis* and *Echinococcus vogeli* (7, 9). The data by Hulsmeier et al. also suggest that both cores can be decorated with a Galp1–4 on their Galp β 1–3 residue. In the light of our work, this addition is likely the Galp α 1–4 cap, which therefore appears to be added directly onto the cores. In the *E. granulosus* LL, the cap appears to be added only after either core has been elongated with one or more Galp β 1–3 residue(s), thus allowing the biosynthesis of larger *O*-glycans. In addition, the *E. multilocularis* data suggest that the core 2 GlcNAc residue can be decorated with either Galp1–4 or Galp1–4Galp1–4, which by comparison with our data (Figure 3) are probably Galp β 1–4 and Galp α 1–4Galp β 1–4, respectively. Addition of only the Galp β 1–4 residue on GlcNAc would generate a terminal lactosamine. This motif, reported to induce granuloma formation (39), appears to be absent from the *E. granulosus* LL, in which we invariably find that the core 2 GlcNAc residue is either unsubstituted or substituted with the mentioned disaccharide; this holds not only for the glycans elucidated in full but also for the minor glycans analyzed by MS-MS (Supporting Information Table S1; data not shown). Nondecorated GalNAc (i.e., the T_n-antigen) was detected by electrospray MS as an important *O*-glycan in the *E. multilocularis* mucin (21). The T_n-antigen was detected immunochemically in *E. granulosus* tissues, in a study that did not include the cyst wall (40). However, analysis by gas–liquid chromatography of trimethylsialyl derivatives of fractions eluted from the Bio-Gel P4 gel filtration column at elution volumes near that of a GalNAc-ol standard (fractions A–C in Figure 1A) did not reveal the presence of free GalNAc-ol. Therefore, T_n-antigen is either absent or expressed in very low levels in the *E. granulosus* LL. Interestingly, all of the differences between our data and those of Hulsmeier et al. may be explained by different relative activities of the same set of biosynthetic enzymes. It must be stressed that these differences do not necessarily reflect species differences, as the *E. multilocularis* mucin was affinity-purified with a monoclonal antibody of apparently restricted specificity, as discussed below.

Antibodies elicited by hydatid infections or by immunization with *Echinococcus* preparations are directed mainly against carbohydrates and largely T-independent (41–43). LL carbohydrates are clearly relevant in this context, and strongly bound host immunoglobulins are abundant in the LL (44). However, the specificities of antibodies against *Echinococcus* carbohydrates are not known. Part of the antibodies bound to LL could be directed

against the nondecorated core 1: this constitutes the tumor-associated T_r-antigen, for which there are natural antibodies in healthy humans (reviewed in ref 45). Other antibodies could be directed against the Galp α 1–4Galp β 1–3Gal motif found in products E3, F2, G2, and G7 (and probably further glycans), as hydatid human sera observed to precipitate the LL “mucopolysaccharide” were found to react with an epitope inhibitable by α -Gal but different from the P₁ determinant (20). Either the Galp α 1–4Galp β 1–3Gal motif or the Galp α 1–4Galp β 1–4GlcNAc (P₁) motif could be the target of monoclonal antibody E492, raised against protoscoleces (larval worms), but reactive with the *E. granulosus* LL, and which is inhibitable by Galp α 1–4Gal (41, 46). The monoclonal antibody Em2(G11), used to purify the *E. multilocularis* mucin mentioned (21), reacts with a carbohydrate epitope that is tissue- and species-specific (7, 47). Therefore, the target *O*-glycan may be speculated to be core 2 decorated with what is likely Galp β 1–4, encompassing the probable lactosamine motif apparently absent from the *E. granulosus* LL. The Em2(G11) epitope probably has a restricted expression even in *E. multilocularis*, as opposed to a wider (and cross-species) expression of the E492 epitope; this would explain that *E. multilocularis* material affinity-purified with Em2(G11) reacts readily with E492 while the opposite is not true (46).

The LL is the host-exposed surface of the hydatid cyst, and the dominant components of the LL are the mucin *O*-glycans elucidated in this work. These, and apparently also the rest of the quantitatively significant carbohydrates of the LL, are both related and simple from the structural point of view. Thus, for all of the complexity expected of an entire helminth parasite stage, the hydatid cyst exposes to the host only a few different abundant molecular motifs. This may simplify the understanding of how this parasite induces, as mentioned, a noninflammatory response. A carbohydrate-rich fraction strongly inhibiting splenocyte proliferation *in vitro* is purified from *E. multilocularis* by the antibody E492 (46), in all likelihood specific for one of the carbohydrate motifs described in the present report.

ACKNOWLEDGMENT

The authors are grateful to the staff of Unidad de Proteómica y Bioquímica Analíticas, Instituto Pasteur, Montevideo, Uruguay, for support with MALDI-TOF MS, as well as help with freeze-drying. They are also grateful to Alejandra Guerra (Instituto de Higiene, Montevideo, Uruguay) for monosaccharide analyses and to Orlando A. Agrellos Filho (IBCCF, UFRJ) for technical support. The authors thank Cecilia Fernández (Faculty of Chemistry, Montevideo, Uruguay) for expert advice with the *E. granulosus* transcriptome.

SUPPORTING INFORMATION AVAILABLE

Table S1, MALDI-TOF-TOF analysis of minor *O*-glycans; Table S2, NMR assignments of products probably arising from *in vitro* reactions. This material is available free of charge via the Internet at <http://pubs.acs.org>.

REFERENCES

1. Wührer, M., and Geyer, R. (2006) Glycoconjugate structures, in *Parasitic Flatworms: Molecular Biology, Biochemistry, Immunology and Physiology* (Maule, A. G., and Marks, N. J., Eds.) pp 408–422, CAB International, Wallingford.
2. Diaz, A., and Allen, J. E. (2007) Mapping immune response profiles: the emerging scenario from helminth immunology. *Eur. J. Immunol.* 37, 3319–3326.

3. Ferreira, A. M., Irigoín, F., Breijo, M., Sim, R. B., and Díaz, A. (2000) How *Echinococcus granulosus* deals with complement. *Parasitol. Today* 16, 168–172.
4. Terrazas, L. I. (2008) The complex role of pro- and anti-inflammatory cytokines in cysticercosis: immunological lessons from experimental and natural hosts. *Curr. Top. Med. Chem.* 8, 383–392.
5. Zacccone, P., Fehervari, Z., Phillips, J. M., Dunne, D. W., and Cooke, A. (2006) Parasitic worms and inflammatory diseases. *Parasite Immunol.* 28, 515–523.
6. Thompson, R. C. A. (1995) Biology and systematics of *Echinococcus*, in *Echinococcus and Hydatid Disease* (Thompson, R. C. A., and Lymbery, A. J., Eds.) pp 1–50, CAB International, Wallingford.
7. Ingold, K., Dai, W., Rausch, R. L., Gottstein, B., and Hemphill, A. (2001) Characterization of the laminated layer of *in vitro* cultivated *Echinococcus vogeli* metacestodes. *J. Parasitol.* 87, 55–64.
8. Gottstein, B., and Hemphill, A. (2008) *Echinococcus multilocularis*: the parasite-host interplay. *Exp. Parasitol.* 119, 447–452.
9. Ingold, K., Gottstein, B., and Hemphill, A. (2000) High molecular mass glycans are major structural elements associated with the laminated layer of *in vitro* cultivated *Echinococcus multilocularis* metacestodes. *Int. J. Parasitol.* 30, 207–214.
10. Richards, K. S., Arme, C., and Bridges, J. F. (1983) *Echinococcus granulosus equinus*: an ultrastructural study of the laminated layer, including changes on incubating cysts in various media. *Parasitology* 86, 399–405.
11. Casaravilla, C., Brearley, C., Soule, S., Fontana, C., Veiga, N., Bessio, M. I., Ferreira, F., Kremer, C., and Díaz, A. (2006) Characterization of myo-inositol hexakisphosphate deposits from larval *Echinococcus granulosus*. *FEBS J.* 273, 3192–3203.
12. Irigoín, F., Casaravilla, C., Iborra, F., Sim, R. B., Ferreira, F., and Díaz, A. (2004) Unique precipitation and exocytosis of a calcium salt of myo-inositol hexakisphosphate in larval *Echinococcus granulosus*. *J. Cell. Biochem.* 93, 1272–1281.
13. Irigoín, F., Ferreira, F., Fernández, C., Sim, R. B., and Díaz, A. (2002) myo-Inositol hexakisphosphate is a major component of an extracellular structure in the parasitic cestode *Echinococcus granulosus*. *Biochem. J.* 362, 297–304.
14. Andrade, M. A., Siles-Lucas, M., Espinoza, E., Perez Arellano, J. L., Gottstein, B., and Muro, A. (2004) *Echinococcus multilocularis* laminated-layer components and the E14t 14-3-3 recombinant protein decrease NO production by activated rat macrophages *in vitro*. *Nitric Oxide* 10, 150–155.
15. Irigoín, F., Laich, A., Ferreira, A. M., Fernández, C., Sim, R. B., and Díaz, A. (2008) Resistance of the *Echinococcus granulosus* cyst wall to complement activation: analysis of the role of InsP₆ deposits. *Parasite Immunol.* 30, 354–364.
16. Steers, N. J., Rogan, M. T., and Heath, S. (2001) In-vitro susceptibility of hydatid cysts of *Echinococcus granulosus* to nitric oxide and the effect of the laminated layer on nitric oxide production. *Parasite Immunol.* 23, 411–417.
17. Kilejian, A., Sauer, K., and Schwabe, C. (1962) Host-parasite relationship in Echinococcosis. VIII. Infrared spectra and chemical composition of the hydatid cyst. *Exp. Parasitol.* 12, 377–392.
18. Kilejian, A., and Schwabe, C. W. (1971) Studies on the polysaccharides of the *Echinococcus granulosus* cyst, with observations on a possible mechanism for laminated membrane formation. *Comp. Biochem. Physiol. B* 40, 25–36.
19. Korc, I., Hierro, J., Lasalvia, E., Falco, M., and Calcagno, M. (1967) Chemical characterization of the polysaccharide of the hydatid membrane of *Echinococcus granulosus*. *Exp. Parasitol.* 20, 219–224.
20. Russi, S., Siracusano, A., and Vicari, G. (1974) Isolation and characterization of a blood P1 active carbohydrate antigen of *Echinococcus granulosus* cyst membrane. *J. Immunol.* 112, 1061–1069.
21. Hulsmeier, A. J., Gehrig, P. M., Geyer, R., Sack, R., Gottstein, B., P., D., and P., K. (2002) A major *Echinococcus multilocularis* antigen is a mucin-type glycoprotein. *J. Biol. Chem.* 277, 5742–5748.
22. Díaz, A., Ferreira, A., and Sim, R. B. (1997) Complement evasion by *Echinococcus granulosus*: sequestration of host factor H in the hydatid cyst wall. *J. Immunol.* 158, 3779–3786.
23. Díaz, A., Willis, A. C., and Sim, R. B. (2000) Expression of the proteinase specialized in bone resorption, cathepsin K, in granulomatous inflammation. *Mol. Med.* 6, 648–659.
24. Davies, M., Smith, K. D., Harbin, A. M., and Hounsell, E. F. (1992) High-performance liquid chromatography of oligosaccharide alditols and glycopeptides on a graphitized carbon column. *J. Chromatogr.* 609, 125–131.
25. Jansson, P. E., Kenne, L., Liedgren, H., Lindberg, B., and Lunngrén, J. (1976) A practical guide to the methylation analysis of carbohydrates. *Chem. Commun. Univ. Stockholm* 8, 1–74.
26. Sweeley, C. C., Bentley, R., Makita, M., and Wells, W. W. (1963) Gas-liquid chromatography of trimethylsilyl derivatives of sugars and related substances. *J. Am. Chem. Soc.* 85, 2497–2507.
27. Gutiérrez, A. L., Farage, L., Melo, M. N., Mohana-Borges, R. S., Guerardel, Y., Coddeville, B., Wieruszkeski, J. M., Mendonça-Prevato, L., and Prevato, J. O. (2007) Characterization of glycoinositolphosphoryl ceramide structure mutant strains of *Cryptococcus neoformans*. *Glycobiology* 17, 1C–11C.
28. Morelle, W., and Michalski, J. C. (2007) Analysis of protein glycosylation by mass spectrometry. *Nat. Protoc.* 2, 1585–1602.
29. Jones, C., Todeschini, A. R., Agrellos, O. A., Prevato, J. O., and Mendonça-Prevato, L. (2004) Heterogeneity in the biosynthesis of mucin O-glycans from *Trypanosoma cruzi* tulahuén strain with the expression of novel galactofuranosyl-containing oligosaccharides. *Biochemistry* 43, 11889–11897.
30. Thornalley, P. J., Langborg, A., and Minhas, H. S. (1999) Formation of glyoxal, methylglyoxal and 3-deoxyglucosone in the glycation of proteins by glucose. *Biochem. J.* 344 (Part 1), 109–116.
31. Persat, F., Bouhours, J. F., Mojon, M., and Petavy, A. F. (1992) Glycosphingolipids with Gal beta 1–6Gal sequences in metacestodes of the parasite *Echinococcus multilocularis*. *J. Biol. Chem.* 267, 8764–8769.
32. Khoo, K. H., Nieto, A., Morris, H. R., and Dell, A. (1997) Structural characterization of the N-glycans from *Echinococcus granulosus* hydatid cyst membrane and protoscoleces. *Mol. Biochem. Parasitol.* 86, 237–248.
33. Cameron, G. L., and Staveley, J. M. (1957) Blood group P substance in hydatid cyst fluids. *Nature* 179, 147–148.
34. Makni, S., Ayed, K. H., Dalix, A. M., and Oriol, R. (1992) Immunological localization of blood pl antigen in tissues of *Echinococcus granulosus*. *Ann. Trop. Med. Parasitol.* 86, 87–88.
35. Dennis, R. D., Baumeister, S., Irmer, G., Gasser, R. B., and Geyer, E. (1993) Chromatographic and antigenic properties of *Echinococcus granulosus* hydatid cyst-derived glycolipids. *Parasite Immunol.* 15, 669–681.
36. King, M. J. (1994) Blood group antigens on human erythrocytes—distribution, structure and possible functions. *Biochim. Biophys. Acta* 1197, 15–44.
37. Hokke, C. H., Deelder, A. M., Hoffmann, K. F., and Wührer, M. (2007) Glycomics-driven discoveries in schistosome research. *Exp. Parasitol.* 117, 275–283.
38. Freire, T., Fernández, C., Chalar, C., Maizels, R. M., Alzari, P., Osinaga, E., and Robello, C. (2004) Characterization of a UDP-N-acetyl-D-galactosamine:polypeptide N-acetylgalactosaminyltransferase with an unusual lectin domain from the platyhelminth parasite *Echinococcus granulosus*. *Biochem. J.* 382, 501–510.
39. Van de Vijver, K. K., Deelder, A. M., Jacobs, W., Van Marck, E. A., and Hokke, C. H. (2006) LacdiNAc- and LacNAc-containing glycans induce granulomas in an *in vivo* model for schistosome egg-induced hepatic granuloma formation. *Glycobiology* 16, 237–243.
40. Alvarez Errico, D., Medeiros, A., Míguez, M., Casaravilla, C., Malgor, R., Carmona, C., Nieto, A., and Osinaga, E. (2001) O-glycosylation in *Echinococcus granulosus*: identification and characterization of the carcinoma-associated T_n antigen. *Exp. Parasitol.* 98, 100–109.
41. Baz, A., Richieri, A., Puglia, A., Nieto, A., and Dematteis, S. (1999) Antibody response in CD4-depleted mice after immunization or during early infection with *Echinococcus granulosus*. *Parasite Immunol.* 21, 141–50.
42. Dai, W. J., Hemphill, A., Waldvogel, A., Ingold, K., Deplazes, P., Mossmann, H., and Gottstein, B. (2001) Major carbohydrate antigen of *Echinococcus multilocularis* induces an immunoglobulin G response independent of alpha beta⁺ CD4⁺ T cells. *Infect. Immun.* 69, 6074–6083.
43. Sterla, S., Sato, H., and Nieto, A. (1999) *Echinococcus granulosus* human infection stimulates low avidity anticarbohydrate IgG₂ and high avidity anti-peptide IgG₄ antibodies. *Parasite Immunol.* 21, 27–34.
44. Varela-Díaz, V. M., and Coltorti, E. A. (1973) The presence of host immunoglobulins in hydatid cyst membranes. *J. Parasitol.* 59, 484–488.
45. Yu, L. G. (2007) The oncofetal Thomsen-Friedenreich carbohydrate antigen in cancer progression. *Glycoconjugate J.* 24, 411–420.
46. Walker, M., Baz, A., Dematteis, S., Stettler, M., Gottstein, B., Schaller, J., and Hemphill, A. (2004) Isolation and characterization of a secretory component of *Echinococcus multilocularis* metacestodes potentially involved in modulating the host-parasite interface. *Infect. Immun.* 72, 527–536.
47. Deplazes, P., and Gottstein, B. (1991) A monoclonal antibody against *Echinococcus multilocularis* Em2 antigen. *Parasitology*. 103 (Part 1), 41–49.

48. Domon, B., and Costello, C. E. (1988) A systematic nomenclature for carbohydrate fragmentations in FAB-MS/MS spectra of glycoconjugates. *Glycoconjugate J.* 5, 397–409.
49. Wieruszkeski, J. M., Michalski, J. C., Montreuil, J., Strecker, G., Peter-Katalinic, J., Egge, H., van Halbeek, H., Mutsaers, J. H., and Vliegthart, J. F. (1987) Structure of the monosialyl oligosaccharides derived from salivary gland mucin glycoproteins of the Chinese swiftlet (genus *Collocalia*). Characterization of novel types of extended core structure, Gal beta(1–3)[GlcNAc beta(1–6)] GalNAc alpha(1–3)GalNAc(-ol), and of chain termination, [Gal alpha(1–4)]_{0–1}[Gal beta(1–4)]₂GlcNAc beta(1–). *J. Biol. Chem.* 262, 6650–6657.